Electrical Conductivity of High Pressure Ionized Argon

C. Goldbach and G. Nollez
Institut d'Astrophysique, Paris, France

S. Popović and M. Popović
Institute of Physics, Beograd, Yugoslavia

Z. Naturforsch. **33a**, 11–17 (1978); received April 21, 1977

In order to investigate some properties of a medium with a low number of particles in a Debye sphere, the electrical conductivity of high-pressure ionized Argon has been measured. A special emphasis is laid on the so-called "non-ideality" effects in the collective behaviour of charged particles. A kind of threshold for these effects is observed at $n_D \leqq 4$. The observed asymptotic behaviour of the screening parameter indicates that heavy charged particles have the same influence on the screening mechanism as electrons. The experimental values of the electrical conductivity are in excellent agreement with similar recent measurements.

Introduction

The basic property of ionized gases at pressures exceeding the atmospheric pressure and at temperatures of the order of 1 eV is their nonneutrality in ranges equal to the corresponding Debye length. However the number n_D of charged particles in a sphere with a radius equal to the Debye length r_D is not much greater than unity in this case and the condition which a gaseous medium should satisfy to be an ideal "plasma" (after some recent definitions [1])

$$n_D = \frac{4\pi}{3} n r_D^3 \gg 1 \tag{1}$$

is not fulfilled. Here n is the number density of charged particles. The violation of condition (1) implies the fact that the potential energy of the charged particles is not negligible in comparison with their kinetic energy. Transport properties of a medium where relation (1) is not satisfied cannot be correctly described by the binary collision approximation, which is valid for an ideal ionized gas. Therefore a "non ideal" term has been rather often used. A "weakly non ideal" term was sometimes used for media similar to those discussed here [2], i.e. where $n_D \gtrsim 1$.

A correct description of the charged particle interaction in non ideal ionized gases cannot be considered as completely established [3, 4]. The corresponding effective collision frequencies — or effective cross sections — can be derived by use of analytical asymptotic expressions for the collision integrals [5, 6, 7]. All these expressions diverge when the value of the Coulomb logarithm, in the denominator, approaches unity [8]. In this case a standard technique with classical formulae for cross-sections and collision integrals [9] with a shielded Coulomb potential seems to be more appropriate [8]. However in this case the uncertainties concerning the proper cut-off and the influence of dynamic effects cannot be estimated.

On the other hand, an experimental investigation of the charged particle interactions encounters two main difficulties. First, there is no laboratory device which can produce a fully ionized plasma. All laboratory plasma are only partially ionized and the non-ideality effects should be selected from a number of other effects by a careful analysis. Second, the information on elementary interactions has to be deduced from the experimental values of some other macroscopic parameter, for instance the electrical conductivity. These two points have a direct effect on the accuracy and on the reliability of the results. Thus it is to be noted that the electrical conductivity of high-pressure ionized Argon corresponding to stationary [3, 4], or pulsed [10] arc experiments differs in general trend as well as in particular values more than the estimated precision allows.

We present in this paper electrical conductivity measurements, performed in a wall-stabilized stationary argon arc, for pressures up to 20 atm. The experimental data are analyzed in terms of non-ideality effects, i.e. of an effective screening radius, so that information on charged particle interactions may be obtained.

Reprint requests to Dr. M. Popović, Institute of Physics, P.O. Box 57, 11001 Beograd, Yugoslavia.

Experimental Device and Measurements

a) The High-Pressure Arc

The high-pressure wall-stabilized arc used in this experiment is described in Ref. [11]. The plasma channel (length: 70 mm; diameter: 5 mm) is inducted within six electrically insulated copper plates (thickness: 10 mm). The plates are water-cooled (water pressure about 2 atm) and specially designed to withstand a large pressure difference between the working gas and the cooling water. The arc is burning between two water-cooled tungsten cylinders and is ignited at atmospheric pressure by establishing contact between the electrodes.

The whole device is operated at the chosen pressure within a high-pressure steel cylinder. Four fused silica windows, located in the side walls and the electrodes, allow either end-on or side-on obervations. The pressure in the chamber is measured by a membrane pressure gauge connected to a digital voltmeter.

The maximum electrical power input is of the order of 5 kW/cm due to the limited efficiency of the cooling system. Within these limits a good plasma stability is achieved over several hours of steady-state operation.

b) Electrical Measurements

The axial electrical field strength is measured as a function of arc current and pressure. Each plate is individually connected to a stepping switch and the voltage drop between two successive plates is measured using a digital voltmeter. The slope of the linear part of the voltage distribution versus the plasma length yields the axial field strength; this method excludes the electrode drops in the plasma field determination. The arc current is measured using a shunt in the power line.

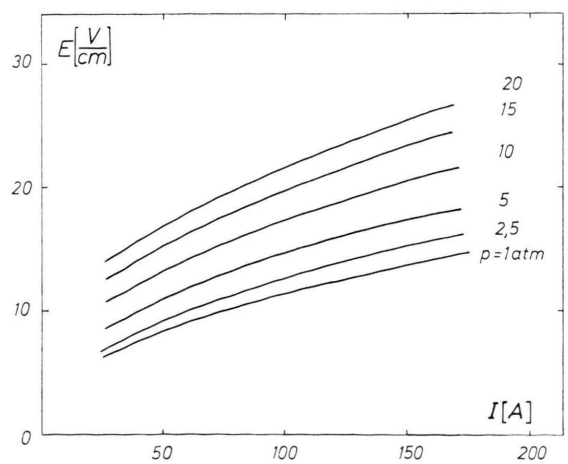

Fig. 1. Axial electrical field strength versus arc current at various pressures.

Figure 1 gives the electrical characteristics at pressures up to 20 atm. The main source of error is related to the finite resistance between two successive plates due to the electrical conductivity of the cooling water. It has been assumed that the axial field strength is constant over the whole correction of the arc.

c) Temperature Distribution

The temperature distribution is deduced from side-on measurements of absolute line intensities. The plasma column is imaged side-on using a spherical mirror (magnification 1:1) on the entrance slit of a grating monochromator (focal length: 2 m, linear dispersion in first order: 8.3 Å/mm; higher orders of the grating are eliminated using filters). The aperture of the optical system is limited to 1:120. The spectrum is photoelectrically recorded and calibrated using a low current carbon arc, which is substituted to the plasma by mechanical displacement on rails. For the absolute spectral radiance of the carbon arc we use the data of Reference [12]. The photomultiplier output signal is measured using a voltage-frequency converter and a frequency-meter with variable integration time.

In order to measure lateral intensity distributions, the plasma image is scanned across the monochromator entrance slit by micrometric displacement of the high-pressure chamber itself. At each lateral position the integration time is put equal to the duration of the grating rotation enabling an entire line profile scanning; the corresponding integrated line intensity is stored on a magnetic tape. The set of data is converted into a radial distribution of the emission coefficient by means of an Abel inversion. The numerical program [13] involves a least-squares smoothing procedure.

The temperature is deduced from the A II $\lambda =$ 4806 Å line at atmospheric pressure. The A I $\lambda =$ 4300 Å and $\lambda = 7147$ Å lines, which remain well isolated at pressures less than 30 atm, are used for higher pressures. Transition probability values are taken from Reference [14]. The influence of reabsorption on the temperature measurements is

discussed in Ref. [15]; it can be considered as negligible for side-on measurements over the full ranges of pressure and temperature investigated.

The agreement between the temperatures deduced from two different lines is within 2%. As an example, Fig. 2 shows mean temperature profiles at various pressures, for a fixed current of 100 amps. For a given pressure, the same temperature is reached at different currents and radial positions; this leads to an improved accuracy in the numerical evaluation of the conductivity. Including the uncertainties in the standard spectral radiance, window transmission, Abel inversion and transition probabilities, the maximum systematic error of the temperature is evaluated to be $\pm 2\%$.

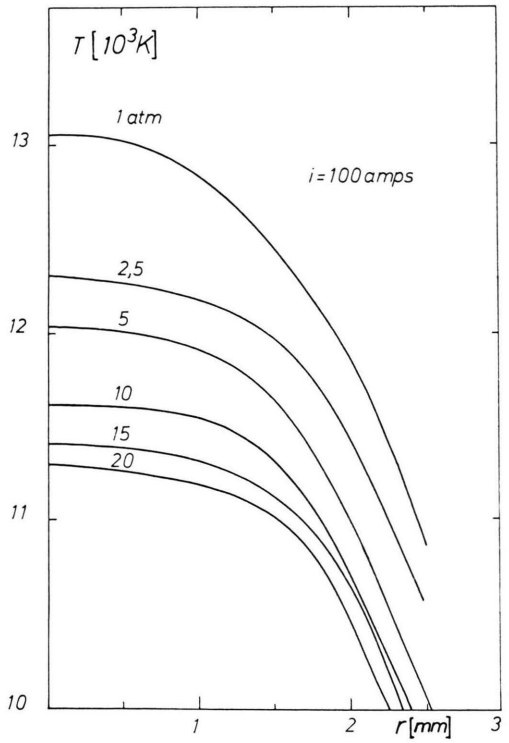

Fig. 2. Radial temperature distributions at 100 amps for various pressures.

Evaluation of the Electrical Conductivity

The electrical conductivity is derived from Ohm's law,

$$I = 2\pi E \int_0^{R_w} \sigma r \, dr \tag{2}$$

by measuring the arc current I, the axial component of the electrical field strength E and the corresponding radial temperature distribution $T(r)$. R_w is the arc radius.

Equation (2) is usually transformed into a Volterra integral equation of the first kind for the unknown conductivity profile $\sigma(r)$ and it can be numerically solved by applying the experimental values for I, E and $T(r)$, with an additional assumption concerning the dependance of σ on T [16–18].

In our treatment, we construct a trial function $\sigma(T)$ following the method described by Shkarofsky et al. [19] for the calculation of the dilute ionized gas conductivity. The construction of $\sigma(T)$ is based on the relation

$$\sigma = n_e e^2 / m \langle \nu \rangle g_\sigma , \tag{3}$$

where

$$\langle \nu \rangle = \frac{4\pi}{3 n_e} \int_0^\infty v^3 (\nu_{ei} + \nu_{ea}) \frac{\partial f_0}{\partial v} \, dv \tag{4}$$

Here ν_{ei} and ν_{ea} are the electron-ion and electron-atom collision frequencies. g_σ is the so-called kinetic function obtained from e-i, e-e and e-a collision matrix elements in the fourth order approximation, using the numerical coefficients tabulated by Hochstim [20]. The number density of electrons, n_e, is obtained from the equilibrium plasma composition, and f_0 is the equilibrium velocity distribution function.

a) Electron-Ion Collisions

A correct description of the interaction between charged particles is one of the important problems concerning the theoretical treatments of ionized gases at elevated pressures. Some difficulties exist also in dilute plasma calculations because the complicated dynamic screening mechanisms cannot be easily introduced in direct calculations. Besides, the models corresponding to elaborated theories cannot be easily verified by experiments.

However models applied in approximate "cut-off" theories yield results which are only numerically equivalent to the theories allowing for the dynamic effects [21], if the influence of heavy charged particles is neglected. Experimental data which were considered also prove that a static Coulomb interaction with collective behaviour of the electrons only can be satisfactory model for calculations of electron transport phenomena in ionized gases [22].

Static screening models with collective behaviour of all charged particles have also been applied in the calculations rather frequently. It is then of some interest to check more directly the validity of these models. The relation between the corresponding effective "dynamic" Debye radius and the Debye radius for static screening in the case of singly ionized gas is

$$r_D^{dyn.} = \sqrt{2}\, r_D^{st.} . \tag{5}$$

Non-ideal effects can also be described in terms of an effective screening radius [23].

Having in mind these circumstances, the cut-off of the Coulomb interaction potential in our construction of the function $\sigma(T)$ is chosen to be at a distance

$$r_S = x\, r_D^{st.} , \tag{6}$$

where x is a free parameter to be obtained so that the whole conductivity function fits the experimental data and Equation (2). The same approach was already used in pulsed arc measurements [24].

In such a model the electron-ion collision frequency has the form

$$\nu_{ei} = n^+ \frac{4\pi}{v^3}\left(\frac{Ze^2}{4\pi\,\varepsilon_0\, m}\right)^2 \ln\lambda , \tag{7}$$

where n^+ is the density of singly charged ions. $\lambda = r_S/b_0$, r_S is defined by (6) and $b_0 = Ze^2/3kT$.

b) Electron-Neutral Collisions

The presence of neutral atoms in the arc disturbs the observation of eventual non-ideality effects. Therefore special care is taken in the estimation of the electron-neutral collision frequency

$$\nu_{ea} = \sum_{n=0}^{n} N_n\, v\, Q_{en} , \tag{8}$$

where N_n is the population of neutrals in the group defined by the principal quantum number n. N_0 is the density of ground state atoms. The summation is taken over all states that are defined as bound after Griem's criterion [25]. Q_{en} are the electron-atom momentum transfer cross-sections, which are introduced from the experimental data using the appropriate fitting formulae in the case of ground state only [26].

The momentum transfer between electrons and excited atoms is classically estimated as a scattering of the electrons on a spherically symetric polarisation potential. Only large impact parameters are taken into account, close collisions are omitted.

The integrals necessary for the calculation of the deflection angle and of the effective cross-section are computed numerically [26]. A long range cut-off is introduced at a distance equal to the mean interparticle distance. The corresponding static polarisabilities of excited states are taken from Reference [27].

Particle number densities necessary for calculations of the effective collision frequencies are deduced from the equilibrium composition equations assuming two-fold ionisation only. Since temperatures below 10000 K will always be present in the outer region of the arc, the difference between the electron (T_e) and the heavy particle (T_a) temperatures is introduced through

$$T_a = T_e - \frac{M}{3k}\left(\frac{eE_{z0}}{m_e\langle v\rangle}\right)^2 , \tag{9}$$

where M is the atom mass and E_{z0} the axial electrical field strength. The state equation is consequently used in the form

$$p = n_e\, kT_e + (n_a + n^+ + n^{++})\, kT_a . \tag{10}$$

Thus an additional iterative procedure is introduced for calculating T_a. First $\langle v\rangle$ is calculated assuming $T_a = T_e$; then the experimental value of E_{z0} is introduced, T_a is calculated from (10) and the whole procedure is repeated.

The only arbitrary step in the construction of $\sigma(T)$ is the choice of the screening radius. With the free parameter x defined by relation (6) the conductivity function is complete. The value of the free parameter has to be determined so that the integral on the right side of Eq. (2) equals the value obtained by electrical measurements.

In that way we have obtained a trial function $\sigma(T)$ as realistic as possible. With the so established procedure the free parameter is no longer only an arbitrary constant which has to be adjusted to reproduce experimental data, but provides also an additional information concerning the interaction between charged particles and the non-ideality effects.

Results and Discussion

The evaluation procedure of the electrical conductivity and the effective screening parameter being rather complicated an exact error analysis

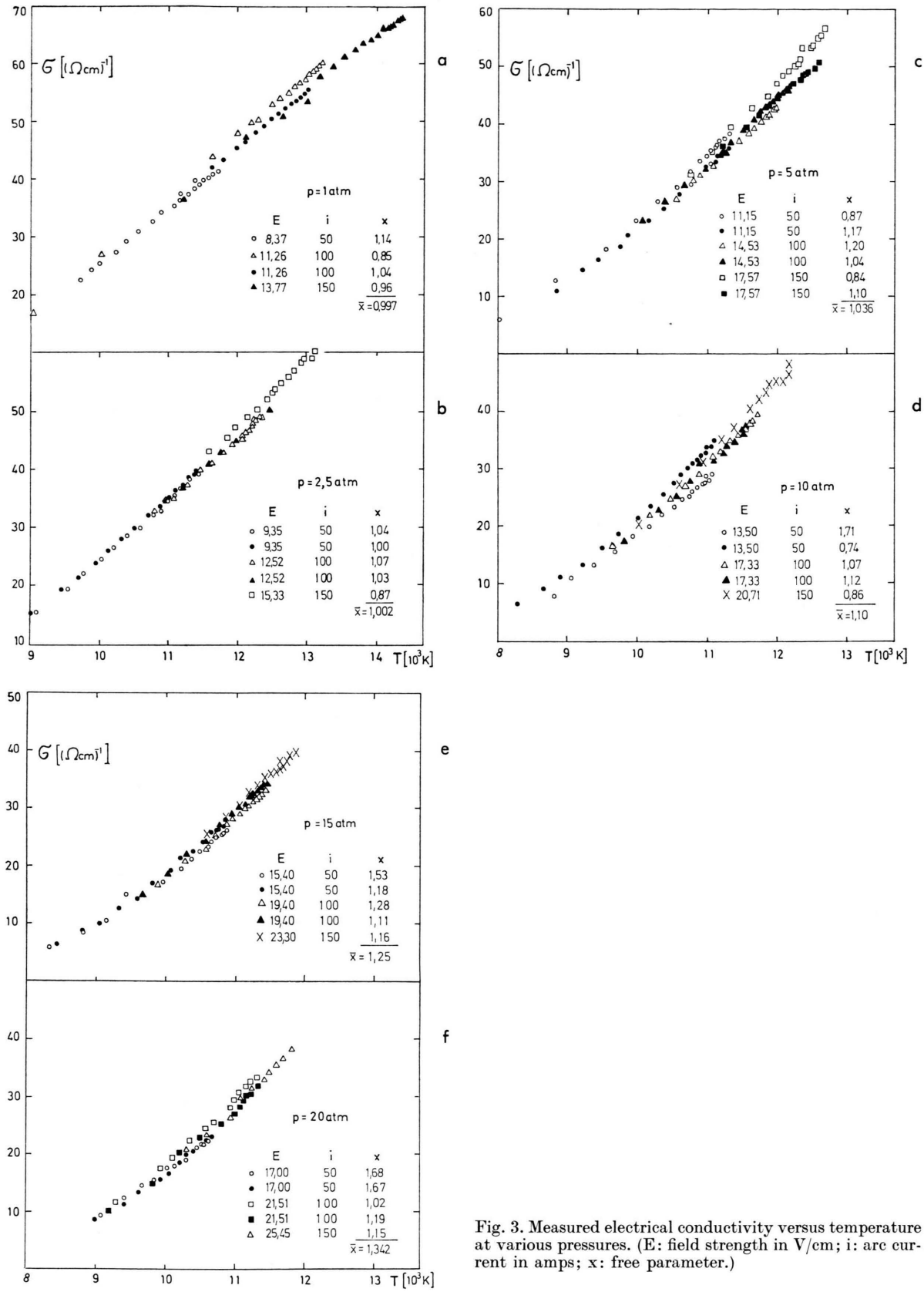

Fig. 3. Measured electrical conductivity versus temperature at various pressures. (E: field strength in V/cm; i: arc current in amps; x: free parameter.)

cannot be performed. It is therefore preferable to vary the input parameters E, I and $T(r)$ and to look for the variations of σ and x. In that way both the precision achieved of the electrical conductivity and the numerical procedure are tested. For the extreme conditions that could be expected from the experiments we obtained variations in x of $\pm 50\%$, which is much more than the scatter of the experimental results.

The electrical conductivity values obtained by the proposed procedure are presented in Fig. 3 and 4 in two forms: as $\sigma(T, p = \text{const})$ and $\sigma(p, T = \text{const})$ functions. Figure 3 may be of interest for the quantitative results.

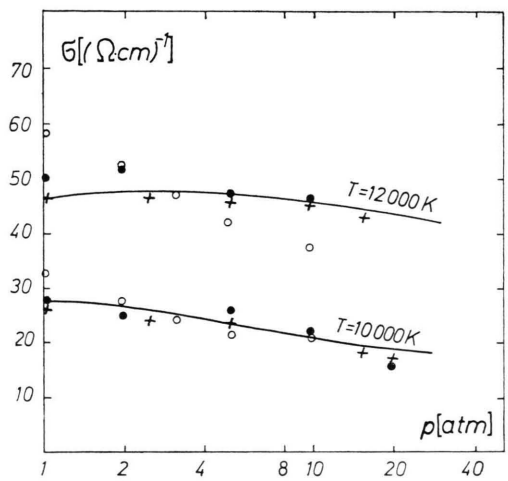

Fig. 4. Measured electrical conductivity versus pressure for two selected temperatures. (+) present work; (○) Kopainski, Ref. [3]; (●) Bauder et al., Ref. [4]; ——— Devoto, Ref. [8] (theory).

The curves display a trend to convex behaviour at elevated pressures which was also observed by Bauder et al. [4].

In Fig. 4 our results are compared with the results of Kopainsky [3], Bauder et al. [4] and theoretical calculations of Devoto [8]. The present results agree very well with the results of Bauder et al. and are at variance with those obtained by Kopainsky at 12000 K.

In Fig. 5 our free parameter, which is the ratio of the effective screening radius to the corresponding Debye length, is plotted as a function of the number of charged particles in a Debye sphere. If the screening of electrons by ions is neglected, the asymptotic value of the free parameter for large n_D values would be $\sqrt{2}$.

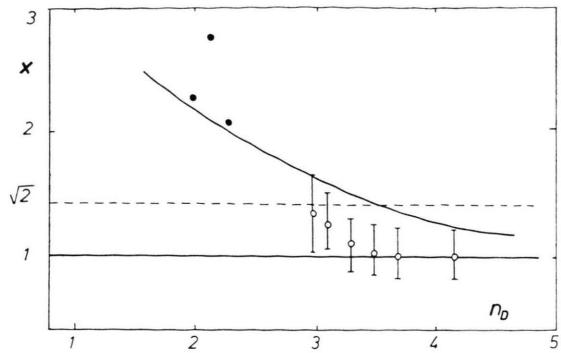

Fig. 5. Screening parameter x versus number of particles in a Debye sphere n_D. (○) present work; (●) Günther et al., Ref. [24]; ----- "dynamic screening" model; ——— Kaklyugin-Norman model (Ref. [23]).

The values of the parameter x presented in Fig. 5 are averaged over several different experimental values for a particular pressure. The error bars represented in the diagram illustrate the dispersion of the experimental values.

In Fig. 5 two models for the treatment of the interactions of charged particles are also shown. The model which includes the screening mechanism by electrons only [8] can be treated as a rough approximation for non ideality effects. The model proposed by Kaklyugin and Norman [23] agrees fairly well with the present results although it is based on somewhat arbitrary considerations.

It is necessary to point out that the definition of the Coulomb logarithm is somewhat arbitrary and depends on the choice of the Debye length as well as on the minimum impact parameter. For instance, the difference between the Coulomb logarithm used here and the value used by Devoto [8] is

$$\ln \lambda = \ln x + \ln \frac{3}{8} + |\ln \lambda|_{\text{Devoto}} \qquad (11)$$

where x is the free parameter. These deviations vary within the range of 15% for the plasma conditions in the present work. They are listed in Table 1.

Table 1. Relative difference between the values of the Coulomb logarithm used in this work and the values used by Devoto [8].

p (atm)	1	2.5	5	10	15	20
(%)	− 7.6	− 7.4	− 3.7	+ 2.5	+ 14.7	+ 17.7

[1] J. Haines, In: Plasma Physics, Ed. B. Ekkeen, London, Inst. Phys. (Cont. Series No. 20) (1974).
[2] P. P. Kulik, AIAA Paper No. 72—414 (1972).
[3] J. Kopainsky, Z. Phys. **248**, 417 (1971).
[4] U. Bauder, R. Devoto, and D. Mukherjee, Phys. Fluids **16**, 2143 (1973).
[5] R. L. Liboff, Phys. Fluids **2**, 40 (1958).
[6] T. Kihara and O. Aono, J. Phys. Soc. Japan **18**, 837 (1963).
[7] R. H. Williams and H. E. Dewitt, Phys. Fluids **12**, 2326 (1969).
[8] R. S. Devoto, Phys. Fluids **16**, 616 (1973).
[9] J. O. Hirschfelder, Ch. F. Curtiss, and R. B. Bird, Molecular Theory of Gases and Liquids, J. Wiley & Sons Inc., New York 1954.
[10] R. Radtke and K. Günther, Proc. XI ICPIG, 274, Prague 1973.
[11] C. Goldbach, G. Nollez, and R. Peyturaux, J. Quant. Spect. & Rad. Transfer **12**, 1089 (1972).
[12] H. Magdeburg and U. Schley, Z. Angew. Phys. **20**, 465 (1966).
[13] C. Fleurier and J. Chapelle, J. Comp. Phys. Comm. **7**, 200 (1974).
[14] H. Nubbemeyer, J. Quant. Spect. & Rad. Transfer **16**, 395 (1976).
[15] C. Goldbach, G. Nollez, and P. Plomdeur, in press in the J. Phys. B.
[16] G. Schmitz and H. J. Patt, Z. Phys. **167**, 163 (1962).
[17] R. S. Devoto and D. Mukherjee, J. Pl. Phys. **9**, 65 (1973).
[18] K. Günther and R. Radtke, Beitr. Plasmaphys. **12**, 63 (1972).
[19] I. P. Shkarofsky, T. W. Johnson, and M. P. Bachynski, The Particle Kinetics of Plasmas, Addison Wesley Pub. Comp., Reading Mass., 1966.
[20] A. R. Hochstim, ed. Kinetic Processes in Gases and Plasmas, Acad. Press, New York 1968.
[21] H. S. Hahn, E. A. Mason, E. J. Miller, and S. I. Sedler, J. Pl. Phys. **7**, 285 (1972).
[22] J. E. Viegas, Phys. Fluids **16**, 616 (1973).
[23] A. S. Kaklyugin and G. E. Norman, Teplofiz. Vysok. Temp. **11**, 238 (1973).
[24] K. Günther, M. M. Popović, S. S. Popović, and R. Radtke, J. Phys. D **9**, 1139 (1976).
[25] H. R. Griem, Plasma Spectroscopy, McGraw Hill, New York 1964.
[26] M. Popović, S. Popović, and S. Vuković, Fizika **6**, 29 (1974).
[27] W. F. Hug, A. B. Cambell, and R. S. Tankin, ARL Report No. 67-0218, 1973.